LA-UR- 00-205

Title: CROSS-SECTIONAL MAPPING OF RESIDUAL STRESSES
BY MEASURING THE SURFACE CONTOUR AFTER A CUT

Author(s): Michael B. Prime, ESA-EA

Los Alamos
NATIONAL LABORATORY

Cross-Sectional Mapping of Residual Stresses by Measuring the Surface Contour After a Cut

M. B. Prime
Technical Staff Member, Member ASME
Engineering Sciences & Applications Division
Los Alamos National Laboratory
Los Alamos, NM 87545
prime@lanl.gov

Abstract

A powerful new method for residual stress measurement is presented. A part is cut in two, and the contour, or profile, of the resulting new surface is measured to determine the displacements caused by release of the residual stresses. Analytically, for example using a finite element model, the opposite of the measured contour is applied to the surface as a displacement boundary condition. By Bueckner's superposition principle, this calculation gives the original residual stresses normal to the plane of the cut. This "contour method" is more powerful than other relaxation methods because it can determine an arbitrary cross-sectional area map of residual stress, yet more simple because the stresses can be determined directly from the data without a tedious inversion technique. The new method is verified with a numerical simulation, then experimentally validated on a steel beam with a known residual stress profile.

Introduction

With relaxation methods, residual stresses are determined from deformations measured after material removal. Analytical complexity generally limits such techniques to determination of one-dimensional (1-D) stress variations. For example, in the hole drilling [1] and crack compliance [2] methods, strains measured at incremental hole or slot depths, z, may be expressed as

$$e(z) = \int_0^z A(z,Z)\, s(Z)\, dZ, \qquad (1)$$

where A is a function of geometry and material properties that is determined using complex analytical solutions or an extensive series of finite element (FE) calibrations. The techniques used to *invert* this equation for the residual stress as a function of depth, $\sigma(z)$, are complex and time-consuming. Furthermore, at least for hole drilling, the inversion becomes unstable at relatively shallow depths because measured surface strains are insufficient to uniquely determine internal stresses.

Complex 2-D or 3-D spatial variations of residual stress are even more difficult to measure with current relaxation methods. One needs to cut a specimen into many pieces and take many deformation measurements. Even with all of that experimental effort, the analysis to solve the inverse problem for the original residual stresses is often prohibitively complex.

Fundamentally, the analytical complexity and need for an inverse solution occurs because current methods use deformations measured remote from the location of stress relief, i.e., on a pre-existing free surface. A mathematical representation of the geometrical separation between the location of stress relief and the location of deformation measurement is given by the function A in Eq. (1).

The new relaxation technique presented in this work can determine 2-D

variations in residual stress *directly* from the measured deformations. The direct solution is possible because deformation is measured on the surface created by a cut, the location of stress relief, rather than on a pre-existing free surface. Hence, the analysis to solve for the stresses from the measurements is exceedingly simple.

The only common methods that can measure similar 2-D stress maps have significant limitations [3]. The neutron diffraction method is nondestructive but sensitive to microstructural changes [4], time consuming, and limited in maximum specimen size, about 50 mm, and minimum spatial resolution, about 1 mm. Sectioning methods [5,6] are experimentally cumbersome, analytically complex, error prone, and have limited spatial resolution, about 1 cm.

The new relaxation technique for measuring residual stress described in this work is referred to as the "contour method." This paper first describes the theory behind the contour method. Next, this new method is verified using an FE simulation and then experimentally validated on a bent beam specimen. Finally, practical considerations and future applications are discussed.

Theory

The contour method for measuring residual stresses is based on a variation of Bueckner's superposition principle [7]. Figure 1 presents an illustration in 2-D for simplicity, although the principle applies equally in 3-D. In **A**, one starts with the undisturbed part containing the residual stresses to be determined. In **B**, the part has been cut in two and has deformed because of the residual stresses released by the cut. In **C**, the free surface created by the cut is forced back to its original shape. Superimposing the stress state in **B** with the change in stress from **C** gives the original residual stresses throughout the part. This superposition principle assumes that the material behaves elastically during the relaxation of residual stress and that the material removal process does not introduce stresses of sufficient magnitude to affect the measured displacements.

Proper application of this superposition principle allows one to experimentally determine the residual stresses along the plane of the cut. Experimentally, the contour of the free surface is measured after the cut. Analytically, the surface of a stress-free model is forced back to its original configuration as in step **C**. Because the stresses in **B** are unknown, one cannot obtain the original stresses throughout the body. However, the stresses normal to the free surfaces in **B** must be zero. Therefore, step **C** by itself will give the correct stresses along the plane of the cut.

The described superposition principle uniquely determines the original s_x and t_{xy} (and t_{xz} in the 3-D case) residual stress distribution on the plane of the cut. The analytical solution, step **C**, specifies conditions on all boundaries of the body: displacements are specified on the cut plane, and the remaining boundaries are stress free. Also, the body forces are zero throughout the body. Therefore, by Kirchoff's boundary value theorem [8], the solution for the stress state in the elastic body is unique. Conversely, because Bueckner's superposition principle tells us that the solution is correct, only one original distribution of s_x, t_{xy}, and t_{xz} on the cut plane can produce a given set of displacements on the boundaries. Bueckner's superposition principle also tells us that the other residual stresses in the body away from the cut plane and the transverse stresses, s_y, s_z, and t_{yz}, on the cut plane will not change the deformations in the cut part, i.e., our measured contour in step **B** of Fig. 1. Therefore, these stresses will not cause errors in the contour method measurements, but the contour method will not uniquely determine these stresses. However, the analytical

solution (step **C** Fig. 1) does uniquely and correctly determine the *change* in all the stresses throughout the part.

In practice, there is an arbitrary displacement in the contour measurement, i.e., the zero is arbitrary. There is also one arbitrary rotation in 2-D and two in 3-D. However, the apparently arbitrary motions can in fact be uniquely determined by the need for the residual stress distribution to satisfy force and moment equilibrium. Furthermore, an FE model used to solve for the stresses accounts for the arbitrary motions automatically, as will be demonstrated later.

Assumptions and Approximations. The assumptions, mentioned above, that the relaxation of residual stresses occurs elastically and the cutting does not induce stresses are common to relaxation methods [3] and have been studied extensively [e.g., 9,10]. However, the contour method requires one unfamiliar assumption: that the cut occurs along a plane that was flat in the original configuration. Because the body will deform slightly as stresses are released during cutting, the validity of this assumption is not certain even if the cut is perfectly straight relative to a laboratory reference frame. In other words, the original plane of the cut may move during the cutting, and the cut may proceed on a different path. However, both the validation experiment and an FE simulation, which are discussed later, show that the flat cut assumption is reasonable if the specimen is constrained adequately during cutting. In fact, a symmetry argument shows that the plane will not move for a zero-width cut made in the center of a symmetrical clamping arrangement. For such a symmetric case, the only deviation from the flat cut assumption is caused by the finite width of the actual cut.

One approximation to the theory is made purely for convenience in the analysis: the deformed shape of the body is not modeled before analytically performing step **C**. The starting point for this step can be a flat surface because the deformations are quite small for engineering materials, and the analysis is linear. The results will be the same, and the analysis is simpler.

An important approximation limits the contour method to measurement of the normal stresses only and not the shear stresses. Measurement of the surface contour only provides information about the displacements in the normal (x) direction, not those in the transverse (y) direction. Therefore, the analytical approximation of step **C** will force the surface back to its original configuration in the x-direction only, leaving the y-displacements unconstrained. If the residual shear stresses were originally zero along the plane of the cut (t_{xy} in Fig. 1, t_{xz} also for the 3-D case), the approximation is exact: Poisson contractions will return the surface to its original y-position, and the calculated stresses will be correct.

In the general case when shear stresses are present on the cut plane, one need only average the contour measured on the two halves of the part to correctly determine the normal stress, s_x. To explain this theoretically, recall that the deformations caused by the release of residual stresses can be evaluated by considering an equivalent surface traction on the cut plane. For a cut surface with the normal in the x-direction only the equivalent surface traction per unit width, $\mathbf{T}$, is given by

$$T_x = -s_x n_x, T_y = -t_{xy} n_x, \quad (2)$$

where $\mathbf{n}$ is the unit surface normal vector, and $n_y = 0$ in this case. Figure 2 illustrates that the normal traction T_x is symmetric with respect to the cut plane, and the transverse traction T_y is anti-symmetric. Therefore, because the problem is elastic and superposition holds, the average of the contours on the two surfaces will give the contour shape as if only the normal stresses were present.

A numerical simulation in the next section of this paper will demonstrate that the above approximations are reasonable and will

3

demonstrate that averaging correctly handles shear stresses.

Previous Research: Although no previous mention of the method proposed in this paper was found in the literature, a few researchers have applied a similar superposition principle for residual stress measurement. However, rather than measuring the contour of the cut surface, they only measured displacements on pre-existing free surfaces, which are insufficient to produce a 2-D stress map. Williams and Stouffer [11] sawed a fatigue-cracked plate in half along the crack line, measured the displacement of a scribed line near the cut, and calculated both residual stresses and crack-closure stresses. Johnson et al. [12] and Joerms [l3] made a partial radial cut into a railroad wheel and measured the relative displacements of points on either side of the slot. The displacements on the interior of the cut surface were merely inferred from the outer surface measurements and then used to solve for the stresses in a 3-D FE model. Lin and Huang's 3-D FE simulation [14] showed that large errors resulted from such simplifications. Dickson et al. [15] measured slot opening on a partial cut in a weld and calculated a 1-D stress profile using a 2-D FE model.

Numerical Verification

FE simulations were used to demonstrate the validity of the approximations required to implement the contour method. Figure 3 shows one of the simulations. A 2×1 beam was modeled using the ABAQUS commercial FE code [16] and a 40×20 mesh of 8-noded, quadratic shape function, plane stress elements (CPS8). The material behavior was isotropic and linear elastic with Poisson's ratio of 0.3. For residual stress normalized to give a peak value of unity, the elastic modulus was taken as 1000 to give $\sigma_{max}/E = 1000$, which is a typical magnitude for structural metals.

Residual stresses were initialized using a user subroutine, and then one FE analysis step was performed to ensure initial equilibrium. To simulate cutting the part in two, a second analysis step removed the elements on the either half of the beam.

The first simulation considered a beam having no shear stresses along the plane of the cut. The axial residual stresses in the central 50% of the length of the beam were given by a simple parabolic distribution that satisfied equilibrium:

$$\boldsymbol{s}_x(y) = 6y^2 - 6y + 1, \quad (3)$$

where the beam thickness goes from $y = 0$ to 1. The stresses in the outer 25% of the beam length on both ends differed from Eq. (3) in order to satisfy equilibrium and the free boundary conditions. Figure 3 shows the left half of the beam after the cut, with the deformations exaggerated by a factor of 400.

Figure 4 shows that applying the contour method to the beam simulation gave the correct results. To apply the superposition principle, a model of the undeformed and unstressed half of the beam was taken from the full mesh. The displacements of the cut surface from Fig. 3 were applied with opposite sign as displacement boundary conditions to the nodes along the cut surface. Applying only the x-displacements, as would be the case with experimental implementation of the contour method, gave the correct stresses along the cut plane. Applying both x- and y-displacements gave identical results because the Poisson contraction automatically resulted in the correct transverse displacements; consequently the y-displacements gave zero constraint forces.

This first simulation confirmed one of the approximations to be used for practical implementation of the contour method. The stress calculation part of the simulation (i.e., step **C** in Fig. 1) started with an undeformed body, rather than with the body deformed in the shape of the measured contour. As

predicted in the Theory section, the correct results were still obtained because the displacements were small.

The second simulation considered a beam with both shear and normal stresses along the plane of the cut. The normal stresses along the plane of the cut were still given by Eq. (3) but were varied in the x-direction to give $\partial s_x(x,y)/\partial x = -s_x$ along the plane of the cut. Combined with the 2-D local equilibrium condition,

$$\frac{\partial s_x}{\partial x} + \frac{\partial t_{xy}}{\partial y} = 0, \qquad (4)$$

and free surface conditions, this $\partial s_x(x,y)/\partial x$ results in a shear stress distribution on the cut plane of

$$t_{xy}(y) = \left(2y^3 - 3y^2 + y\right), \qquad (5)$$

which is shown in Fig. 5 as a "known" stress.

Figure 5 shows that the contour method gives the correct results when shear stresses are present on the cut plane even though only the normal component (x) of the surface contour can be measured experimentally. The results averaged between the two halves of the beam match the known stresses. The individual results from either from the two halves gave a root-mean-square error in the s_x distribution of 0.059, or 5.9% of the peak value. Even though the simulation considered a pessimistic case[1], the errors are reasonably small. These errors are only relevant if one does not measure both halves of the specimen. For completeness, we note that applying both the x- and y-displacements

---

[1] The shear stress magnitudes should not be compared directly to the normal stresses. Because of the free surface condition ($t_{xy} = 0$ for $y = 0,1$) and equilibrium condition [Eq. (4)], the magnitude of $\partial s_x(x,y)/\partial x$ determines the maximum value of shear stress. The simulation of $\partial s_x(x,y)/\partial x = -s_x$ for a specimen with unity thickness represents a decay of s_x from peak magnitudes to zero in one thickness, which is a fairly steep gradient for a part with no discontinuities in cross section.

to the surface on either half of the beam gave the correct results for both normal and shear stresses.

Experimental Validation

Known Residual Stress Specimen. A plastically bent beam was carefully prepared in order to provide a specimen with a known residual stress profile. 43 mm square forged stock of 21Cr-6Ni-9Mn austenitic stainless steel was annealed at 1080°C for one hour and argon quenched. Next, the beam was machined to final shape with a 30 mm × 10 mm minimum cross section. Then the beam was thoroughly stress relieved by heating in a vacuum to 1080°C for 15 minutes and slow cooling at 100°C per hour. The bending was performed in a four-point bend fixture specially designed to ensure pure moment between the inner rollers [17]. The beam was plastically bent to a maximum outer fiber strain of about 0.57 % and then unloaded. Strain and load measurements during bending were used to calculate independent stress-strain curves for loading and unloading in both tension and compression [17]. Finally, superposition of these curves gave the residual stress profile. This method of predicting residual stress profiles has been verified using a variety of experimental techniques [18]. The elastic modulus determined during these tests was 194 GPa, which compares well with the 197 GPa value reported by the manufacturer for annealed material [19].

The analysis based on loads and strains measured during bending provides only a 1-D profile of residual stresses in the beam. A prediction of the full stress map was obtained by implementing the stress-strain curves measured during the bending test into a 3-D FE model.

Experiment. For the contour method, the ideal machining process for separating the part would make a precisely straight cut, would not remove any further material from

5

already cut surfaces, and would not cause any plastic deformation. Wire electric discharge machining (wire EDM) [20] is probably the choice closest to the ideal. In wire EDM, a wire is electrically charged with respect to the workpiece, and spark erosion causes material removal. The cutting is noncontact, whereas conventional machining causes localized plastic deformation from the large contact forces. The part is submerged in temperature-controlled deionized water during cutting, which minimizes thermal deformations. The wire-control mechanisms can achieve positional precision of a fraction of a micrometer, especially for a straight cut. When the conditions are held constant during the cutting, wire EDM cuts with a constant overcut, which is also necessary to make a straight cut. "Overcut" means that the final slot is wider than the wire making the slot.

For this test, the beam was cut with a Mitsubishi SX-10 wire EDM machine and a 100 μm diameter zinc-coated brass wire. "Skim cut" settings, which are normally used for better precision and a finer surface finish, were used because they also minimize any recast layer and cutting-induced stresses [20,21]. Including the overcut, the slot was about 140 μm wide.

As discussed in the Assumptions and Approximations subsection of the Theory section, the original plane of the cut must be constrained from moving as stresses are relaxed during the cutting. Such constraint requires an unconventional clamping arrangement because usually only one side of the workpiece is clamped for wire EDM. Figure 6 shows how the beam was clamped on both sides for this test. Before clamping, the beam and all the clamps were allowed to come to thermal equilibrium in the water tank to assure that no thermal stresses would arise during the cutting.

After cutting, the beam was removed from the clamps, and the contour of the cut surface was measured using a common inspection tool. A coordinate measuring machine (CMM) registers mechanical contact with a touch trigger probe. An optoelectric system using glass scales gives the probe location, which is combined with machine coordinates to locate the surface. Because the CMM uses a probe tip with a finite radius, surface roughness is at least partially filtered out from the measured contour.

For this test, the measurements were taken using a Brown & Sharpe XCEL 765 CMM, which resides in a temperature and humidity controlled inspection laboratory. A 4 mm diameter ruby tip was selected after trial measurements using tips with diameters from 1 mm to 8 mm revealed no significant measurement differences. The machine resolution is 0.1 μm, and the manufacturer reports measurement accuracy of 3.5 μm over the full 500 mm measurement range. However, precision is more relevant than accuracy for this application because the of the small measurement range and the need for only relative, rather than absolute, measurements. The experimental scatter in the contour measurements on the beam indicates a precision of about ±0.5 μm for measurement on the surface cut by wire EDM.

Figure 7 shows the contours measured separately on the cut surfaces from both halves of the beam. The zeros are arbitrary, so the x-direction offset between the two curves is irrelevant. The measurements were taken in the center (z-direction) of the surface, $y = 0$ represents the beginning of the cut, and measurements were taken approximately every 130 μm. For both surfaces, positive x is taken in the outward normal direction; therefore, values that are more positive represent higher regions of the surface. Near the ends of the data range, there is additional noise in the data. The noise may be caused by

6

machining irregularities on the edge or by the CMM's spherical tip going slightly past the actual edge of the part. Therefore, it is uncertain if the data at the edges correctly represents the part shape, and the calculated stress results will not be plotted all the way to the ends.

Measurements were also taken over the full cut surfaces using the CMM and a 50 by 300 grid. Figure 8 shows the measured surface shape. The measured contours were fit to a bivariate Fourier series to smooth out noise in the data, and Fig. 8 plots the fit rather than the raw data because the 15,000 data points are difficult to clearly plot. The noise level in the data and the quality of the fit are very similar to the 1-D measurements shown in Fig. 7.

Calculations and Results. Initial calculations were performed on a 2-D model using the measurements shown in Fig. 7. The half-beam was modeled using 5180 8-noded, quadratic shape function, plane stress elements (CPS8), with the mesh refined near the cut surface using multi-point constraints. A convergence study indicated that this mesh density is well beyond the refinement needed for a converged answer. The material behavior was isotropic linearly elastic with an elastic modulus of 194 GPa and Poisson's ratio of 0.28. As was discussed in the Theory section and verified by the numerical simulation, it was sufficient to model the cut surface as initially flat rather than deformed in the shape of the measured contour. After the data was smoothed using local spline approximations, shown in Fig. 7, the opposite of the measured contour was applied as displacement boundary conditions to the nodes on the surface representing the cut.

Figure 9 shows the exaggerated deformed shape of the FE model. Only one constraint additional to the imposed contour was necessary to prevent rigid-body motions. As discussed previously in the Theory section, the FE solution easily handled the arbitrary displacement and rotation in the measured contour. The movement of the free end of the beam illustrates the rotation necessary to satisfy moment equilibrium and the slight contraction to satisfy force equilibrium.

Figure 10 shows the 1-D residual stress profiles measured by the contour method compared with the prediction from the bend test. The stresses were obtained by post-processing the FE results to obtain s_x at the nodes along the surface representing the cut. The agreement with the prediction is very good, especially considering the low magnitude of residual stresses. Such low residual stresses in a stiff material like steel result in a decreased magnitude of the contour and, therefore, increased errors. The discussion in the Theory section indicates that the difference between sides one and two may be due to the presence of shear stresses. However, the four-point bent beam should have no shear stresses, and such asymmetry may also arise from the cut not being centered between the clamps or other experimental errors.

To illustrate the ability of the contour method to measure a full 2-D cross-sectional stress map, the contour measured on the entire cut surface, Fig. 8, was applied to a 3-D FE model. The half-beam was modeled in ABAQUS using 16,200 20-noded brick elements (C3D20). This mesh gave a 10×30 mesh of elements on the 10 mm $\times$ 30 mm cut surface. The bivariate Fourier series fits to the measured contour data were evaluated at a grid corresponding to the FE nodes, averaged between sides one and two, and then applied as displacement boundary conditions in the FE model. Figure 11 shows the deformed FE model and the three additional displacement constraints that prevented rigid body motions. The rotations of the free end of the beam, visible in Fig. 11, automatically account for the arbitrary rotations in the measured contour.

7

Figure 12 shows the measured 2-D map of residual stresses compared to the bend test prediction. Because of the aforementioned uncertainty in the surface contour measured near the edges of the surface, the contour lines are not plotted all the way to the edges. The agreement between measurement, Fig. 12b, and prediction, Fig. 12a, is good but not excellent. The z-direction curvature in the measured contour, see Fig. 8, resulted in a shift in the calculated stresses towards more compressive values along the center of the surface ($z = 5$).

The agreement between measurement and prediction would have been better if the correct wire had been used during the EDM cutting. The bent beam specimen had been cut using a brass wire coated with zinc oxide, whereas the manufacturer of the EDM machine recommends a bare brass wire. A test cut using the same coated wire was made on a another specimen made of the same steel, but this time the specimen had been stress relieved. The top graph on Fig. 13 shows the contour measured after that cut, which shows a distinct curvature. Because the beam was stress free, the curvature represents the shape of the cut rather than a stress relief effect. Another test cut was made using the same conditions but with a bare brass wire. The middle graph on Fig. 13 shows that the bare brass wire made a cut that was flat to within the measurement resolution.

Figure 12c shows the improved results obtained by correcting for the curvature in the actual cut. Similar or even better results probably could have been obtained without any correction if the bare brass wire had been used for cutting the beam. The correction was made by subtracting the curvature caused by cutting conditions from the measured contour and recalculating the stresses with the FE model. Figure 13 shows the curvature correction compared to both the test cut on the stress free specimen (top graph) and to the typical curvature measured on the bent beam

(bottom graph – from the raw data used to generate Fig. 8). Note that the low region in the top graph of Fig. 13 corresponds to a region that showed visual evidence of corrosion or some other surface damage after EDM cutting, and there was no corresponding region in the bent beam. Therefore, the curvature correction does not follow the low spot.

Discussion

This section discusses several of the more apparent practical issues of the contour method. First we briefly mention that analytical smoothing of any noise in the measured contour is crucial because calculating stress from the displacements amplifies noise in the data.

The contour method is sufficiently sensitive to measure residual stress maps of interest. The beam specimen in this study could be considered a sensitivity test because the stresses were less than 150 MPa and resulted in a contour with only about a 10 μm peak-to-peak magnitude. Residual stresses are often several times greater, the parts are also often larger, and many materials of interest have lower elastic moduli, any of which would give larger contours. Some preliminary measurements on a 38-mm thick butt-welded steel plate gave a contour of about 120 μm peak-to-peak magnitude. However, larger residual stresses could possibly lead to yielding as the stresses are released during cutting. Although the possibly of yielding should be studied in future research, recent experimental studies have shown that, because of strain hardening effects, reverse yielding does not necessarily occur in relaxation measurements even when the residual stresses exceed the nominal yield strength of a material [10].

As presented, the contour method measures only the stress component normal to the cut surface, which is fine for many measurement applications because the normal

stress is often the largest and the main contributor to failure. A 2-D map of one stress component is also generally more than sufficient for validating predictive models, which is a very important use for residual stress measurements.

Nevertheless, it may be possible to extend the contour method to measurements of additional stress components. The same calculation that determines the normal stresses from the measured surface contour, Fig. 2, also determines the *change* in the transverse normal stresses. Hence, adding the remaining transverse stress on the face of the cut, measured for example using x-ray diffraction, would give the original stresses. Other possibilities for measuring multiple stress components include reconstructing 3-D stresses from 2-D measurements on multiple slices [e.g., 22] or using a curved cut such as a hole [23].

Errors can be greatly reduced by correctly clamping the specimen during the cutting. The cut is assumed to occur along a flat plane in the original configuration. However, stress relief can cause this plane to move slightly as the cut progresses. This effect explains why the contour method results in Figs. 10 and 12 slightly underestimate the stress peaks. Further explanation of this effect and how to calculate and correct for it with an FE calculation is postponed to a future publication. For now, we report that when the specimen is clamped on both sides of the cut, the resulting error in the stress distribution is less than 10%, and more sophisticated clamping arrangements could probably reduce the errors further.

The z-direction curvature in the measured surface contour, see Figs. 8 and 13, was likely caused by a common source of inaccuracy in wire EDM machining called "barreling," where more material is removed near the edges of the cut than in the center [20]. Curvature can also be caused by a tensile recast layer, but that would cause curvature in the other direction. Either effect can be minimized by optimizing cutting parameters, such as by cutting more slowly, using high pulse frequencies, and copious cooling the area of the cut by proper flushing [21,24]. The middle graph in Fig. 13 demonstrates that a very flat surface can be cut if care is taken. Note that curvature, if it was present from the cut, would primarily affect the stresses determined near the edges of the surface because that is where such curvature is the greatest.

Conclusions

The contour method for measuring residual stress was experimentally validated using a bent beam specimen. In many ways, the contour method has the potential to surpass other measurement methods in both its ability to measure stresses and its ease of use:

1. The contour method can measure a full 2-D cross-sectional map of the residual stress component normal to the cross section.
2. The residual stress map can be obtained directly from the measured contour; no inverse procedure or assumptions about the stress variations are necessary.
3. The technique is relatively simple experimentally. No strain gages or other instrumentation are required during the testing. The necessary equipment is widely available in machine shops and inspection laboratories.

The contour method also has the potential to measure residual stress maps that are extremely difficult to measure with other techniques, if possible at all. One particularly promising application is welding residual stresses. Microstructural changes in the weld material make neutron diffraction measurements difficult [e.g., 4] but have relatively small effects on the macroscopic elastic properties that would affect contour

method measurements. Another exciting class of applications is parts with geometrically complex cross sections, like railroad rails, forgings, I-beams, extrusions, and castings.

Several practical points should be considered for anyone wishing to apply the contour method. Wire EDM may be the only current method for making the cut that satisfies the assumptions of the contour method. The part should be securely clamped on both sides of the cut (e.g., Fig 6) during cutting. The surface contour should be measured on both halves of the part after cutting, and the results from the two sides should be averaged to minimize errors. Finally, a test cut should be made in a stress-free region of the part and the resulting surface contour measured to quantify or correct for errors in the assumption of a flat cut.

Acknowledgements

References

[1] Schajer, G. S., 1988, "Measurement of Non-Uniform Residual Stresses Using the Hole-Drilling Method," ASME JOURNAL OF ENGINEERING MATERIALS AND TECHNOLOGY, **110**, pp. 338–349.

[2] Cheng, W., and Finnie, I., 1986, "Measurement of Residual Hoop Stress in Cylinders Using the Compliance Method," ASME JOURNAL OF ENGINEERING MATERIALS AND TECHNOLOGY, **108**, pp. 87–92.

[3] Lu, J., James, M., and Roy, G., eds., 1996, *Handbook of Measurement of Residual Stresses*, The Fairmont Press, Inc., Lilburn, Georgia, USA.

[4] Krawitz, A. D., and Winholtz, R. A., 1994, "Use of Position-Dependent Stress-Free Standards for Diffraction Stress Measurements," *Materials Science and Engineering A-Structural Materials Properties Microstructure and Processing*, **185**, pp. 123–130.

[5] Ueda, Y., 1996, "Sectioning Methods," *Handbook of Measurement of Residual Stresses*, J. Lu et al., eds., Fairmont Press, Inc., Lilburn, Georgia, USA, pp. 49–70.

[6] Rybicki, E. F., and Shadley, J. R., 1986, "A 3-Dimensional Finite-Element Evaluation of a Destructive Experimental Method for Determining Through-Thickness Residual Stresses in Girth Welded Pipes," ASME JOURNAL OF ENGINEERING MATERIALS AND TECHNOLOGY, **108**, pp. 99–106.

[7] Bueckner, H. F., 1958, "The Propagation of Cracks and the Energy of Elastic Deformation," *Transactions of the American Society of Mechanical Engineers*, **80**, pp. 1225–1230.

[8] Timoshenko, S. P., and Goodier, J. N., 1970, *Theory of Elasticity*, 3rd Edition, McGraw Hill, Inc., New York, Article 96.

[9] Flaman, M. T., and Herring, J. A., 1985, "Comparison of Four Hole-Producing Techniques for the Center-Hole Residual Stress Measurement Method, *Experimental Techniques*, **9**, 30-32.

[10] Nobre, J. P., Kornmeier, M., Dias, A. M., Scholtes, B., 2000, "Use of the Hole-Drilling Method for Measuring Residual Stresses in Highly Stressed Shot-Peened Surfaces, *Experimental Mechanics*, **40**, 289-297.

[11] Williams, J. F., and Stouffer, D. C., 1979, "An Estimate of the Residual Stress Distribution in the Vicinity of a Propagating Fatigue Crack," *Engineering Fracture Mechanics*, **11**, pp. 547–557.

[12] Johnson, M. R., Robinson, R. R., Opinsky, A. J., Joerms, M. W., and Stone, D. H., 1985, "Calculation of Residual Stresses in Wheels From Saw Cut Displacement Data," Paper 85-WA/RT-17, The American Society of Mechanical Engineers, New York.

[13] Joerms, M. W., 1987, "Calculation of Residual Stresses in Railroad Rails and Wheels from Sawcut Displacement," *Residual Stress in Design, Process and Material Selection, Proceedings ASM's Conference on Residual Stress in Design, Process and Material Selection*, B. Young, ed., ASM International, Materials Park, OH, pp. 205–209.

[14] Lin, K.Y., and Huang, J. S., 1989, "Analysis of Residual Stresses in Railroad Car Wheels Based on Destructive Test Measurements," *Theoretical and Applied Fracture Mechanics*, **12**, pp. 73–86.

[15] Dickson, T. L., Bass, B. R., and McAfee, W. J., 1998, "The Inclusion of Weld Residual Stress in Fracture Margin Assessments of Embrittled Nuclear

Reactor Pressure Vessels," *PVP-373, Fatigue, Fracture, and Residual Stresses*, *Proceedings of the 1998 ASME/JSME Joint Pressure Vessels and Piping Conference,* San Diego, CA, July 26–20, 1998, pp. 387–395.

[16] Hibbitt, Karlsson & Sorensen, Inc., 1998, ABAQUS/Standard User's Manual Version 5.8, Pawtucket, Rhode Island, USA.

[17] Mayville, R. A., and Finnie, I., 1982, "Uniaxial Stress-Strain Curves from a Bending Test," *Experimental Mechanics*, **22**, pp. 197–201.

[18] Prime, M. B,. Rangaswamy, P., Daymond, M. R., and Abeln, T. G., 1998, "Several Methods Applied to Measuring Residual Stress in a Known Specimen," *Proceedings of the SEM Spring Conference on Experimental and Applied Mechanics*, Houston, Texas, June 1–3, 1998, Society for Experimental Mechanics, pp. 497–499.

[19] Armco Inc., 1983, "Armco NITRONIC 40 Bar and Wire," *Product Data Bulletin S-54a*, Middletown, Ohio, USA.

[20] Sommer, C., and Sommer, S., 1997, *Wire EDM Handbook*, Advance Publishing, Inc., Houston, Texas, USA.

[21] Cheng, W., Finnie, I., Gremaud, M., and Prime, M. B., 1994, "Measurement of Near Surface Residual Stresses Using Electric Discharge Wire Machining," ASME JOURNAL OF ENGINEERING MATERIALS AND TECHNOLOGY, **116**, pp. 1–7.

[22] Magiera, J., Orkisz, J., Karmowski, W., 1996, "Reconstruction of Residual-Stresses in Railroad Rails from Measurements Made on Vertical and Oblique Slices," *Wear*, **191**, pp. 78–89.

[23] Leggatt, R. H., Smith, D. J., Smith, S. D., and Faure, F., 1996, "Development and Experimental Validation of the Deep Hole Method for Residual Stress Measurement," *Journal of Strain Analysis for Engineering Design*, **31**, pp. 177–186.

[24] Benedict, G. F., 1987, *Nontraditional Manufacturing Processes*, Marcel Dekker, Inc., New York, USA.

Figure Captions

1. Superposition principle to calculate residual stresses from surface contour measured after cutting a part in two.

2. Surface tractions equivalent to releasing residual stress on cut surface. Normal traction T_x is symmetric about cut plane, transverse T_y is anti-symmetric. Illustrated for $\boldsymbol{s}_x$ negative and $\boldsymbol{t}_{xy}$ positive.

3. Finite element simulation, deformed shape of beam after separating along midplane.

4. Simulated contour method results for residual stress profile of beam with no shear stresses on cut plane.

5. Simulated contour method results from beam with shear stresses along cut plane when only the normal component (x) of surface contour is measured.

6. Clamping arrangement during wire EDM cutting of beam.

7. 1-D surface contour measured on both halves of the cut beam. Zero is arbitrary, so the shift between the two profiles is irrelevant.

8. 2-D surface contour measured on side two of beam, fitted to bivariate Fourier series.

9. 2-D finite element model of beam after measured contour has been applied as displacement boundary condition. For clarity, only a few elements are shown.

10. 1-D residual stress results from contour method measurements on bent beam.

11. 3-D finite element model after measured contour has been applied as displacement boundary condition.

12. Cross-sectional residual stress map from contour method test on bent beam, stresses are in MPa.

13. Measured surface curvature effects depending on cutting conditions. See Fig. 6 for cutting direction.

$\sigma_x(y)$

+ is tension
- is compression
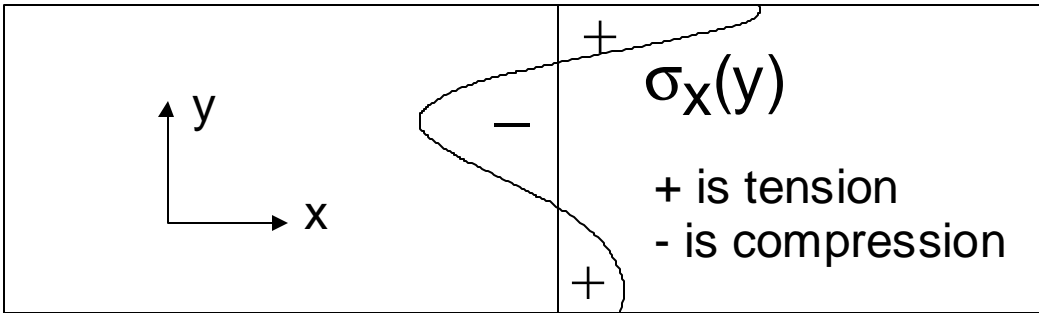
A   Original residual stress distribution.

= B

Part cut in half,
stresses relieved
on face of cut.
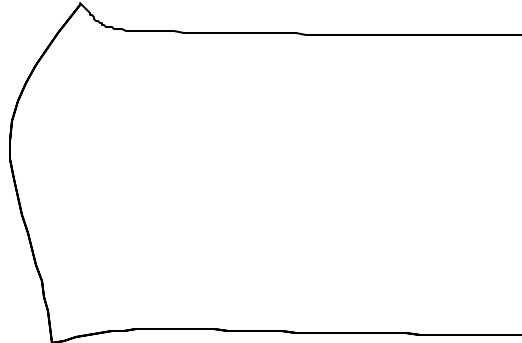
**+ C**

Force cut surface
back to original state.
All stresses back to
original values (A).

cut plane

$n_x=+1$

T_y

T_x

y

x

T_x

T_y

$n_x=-1$

Prime Fig. 2

length 2

cut location

thickness 1

y

x

△ = constraint
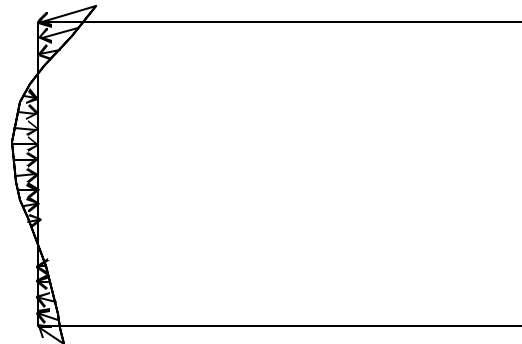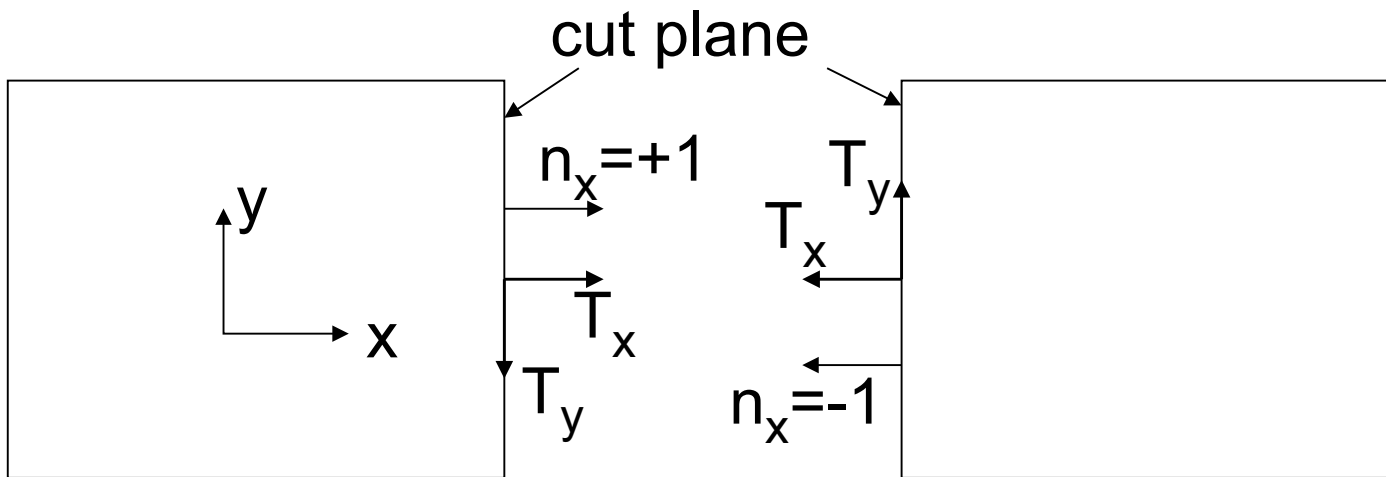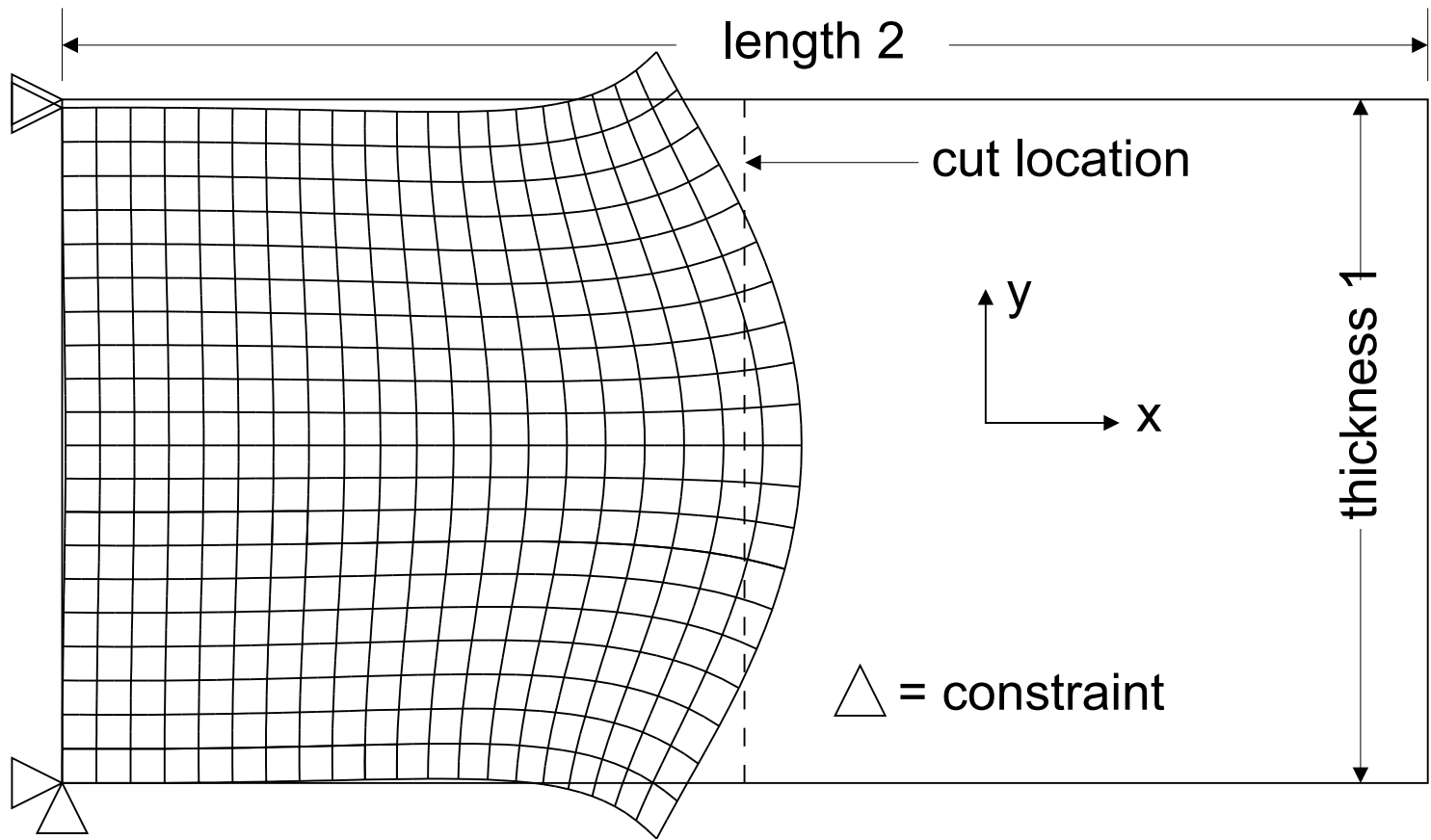
Prime Fig. 3

Prime Fig. 4

Prime Fig. 5

z

x

y

Slot (not
to scale)

EDM wire

10 mm

30 mm

Bolt

Blocks
clamped
to EDM table

Prime Fig. 6

Prime Fig. 7

Prime Fig. 8

additional constraint
to prevent rigid
body movement

Undeformed shape

mesh detail

displacement
boundary conditions

Deformed shape

y

x

Prime Fig. 10

undeformed
shape

z   y

x

additional
constraints
to prevent
rigid body
rotations
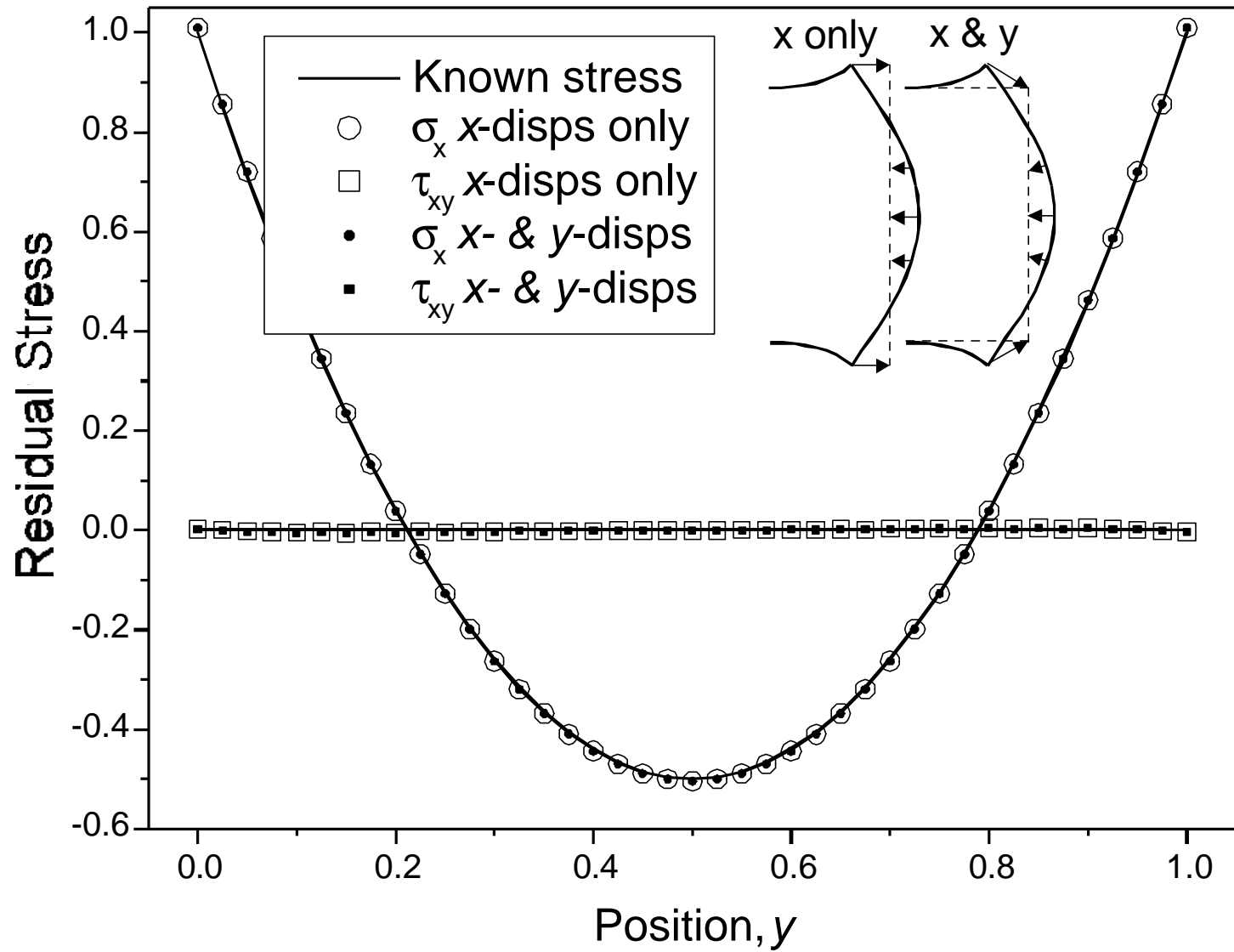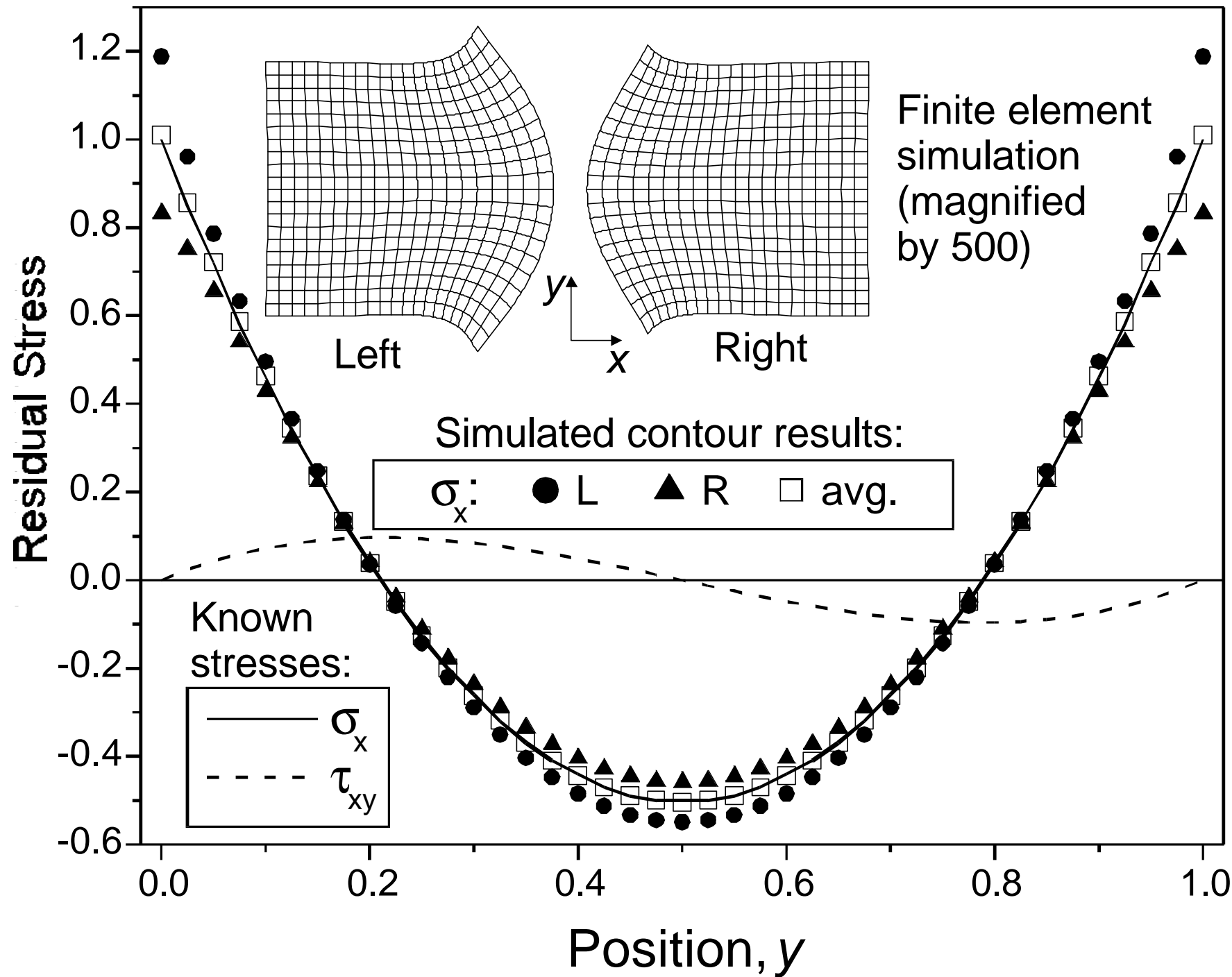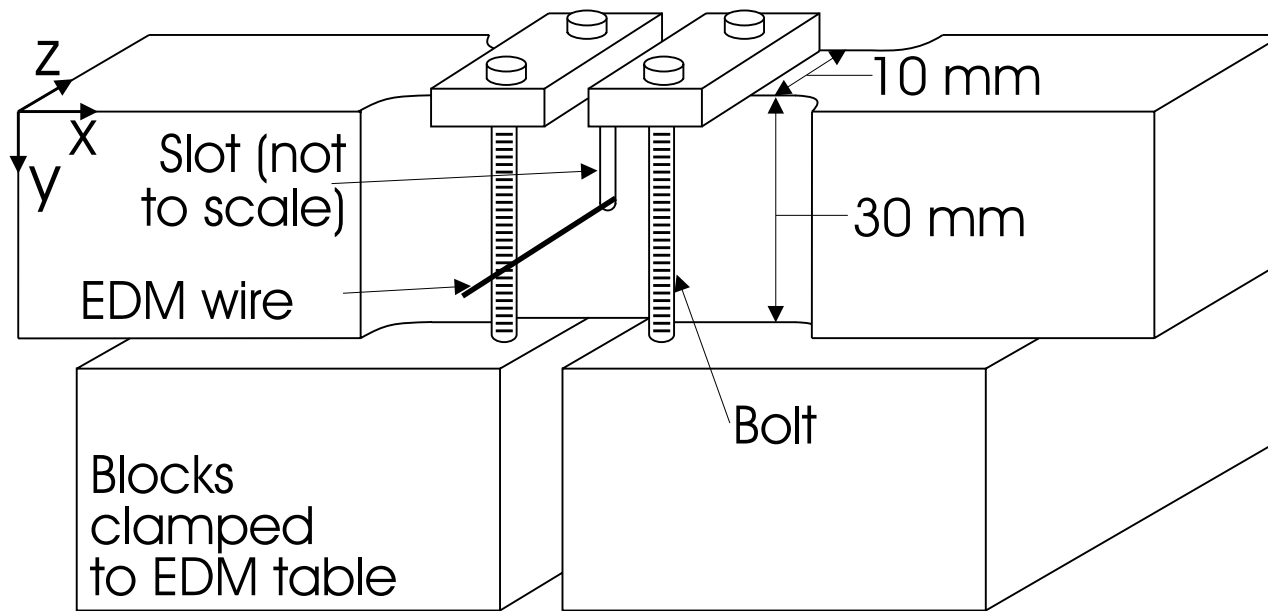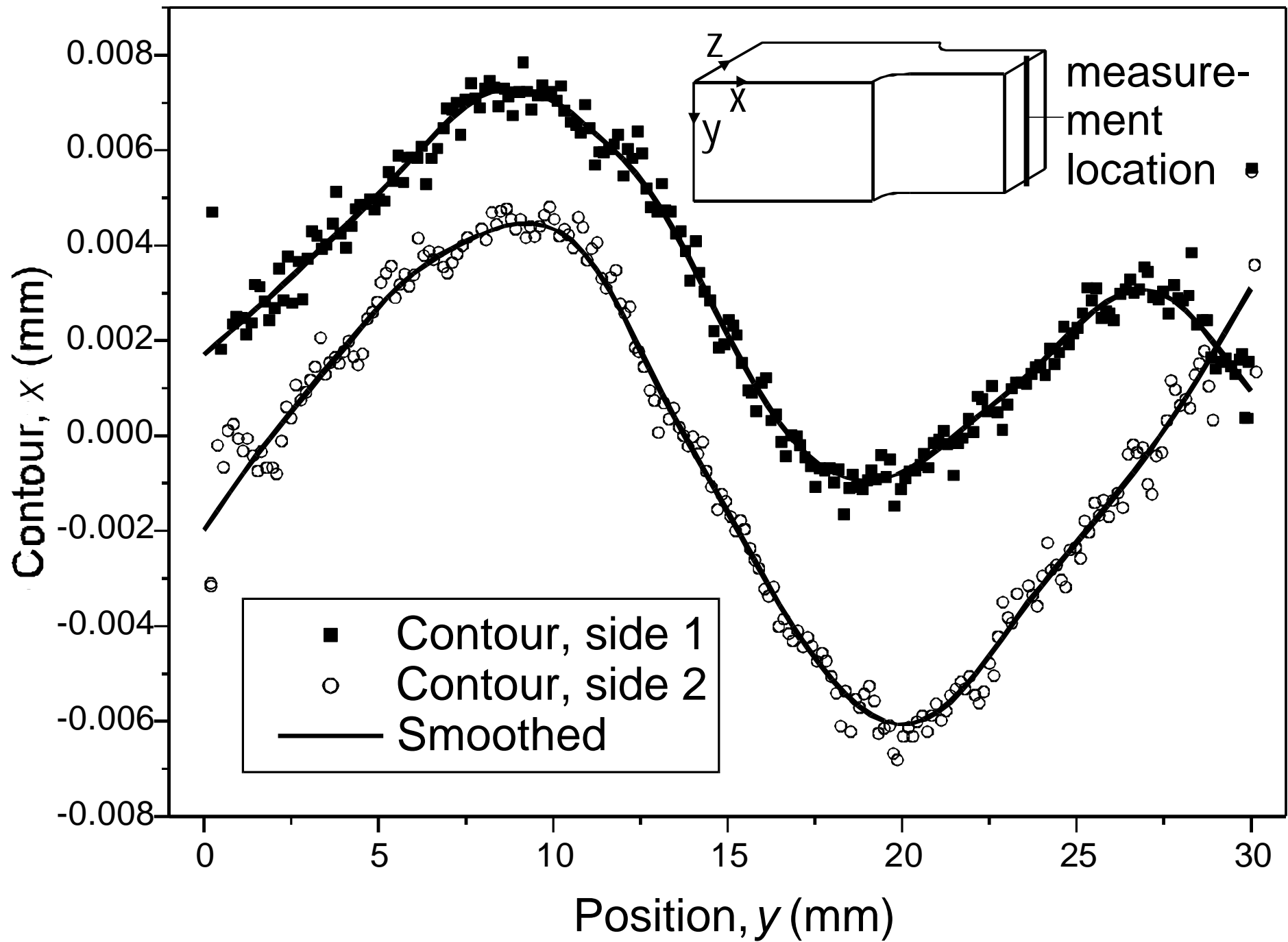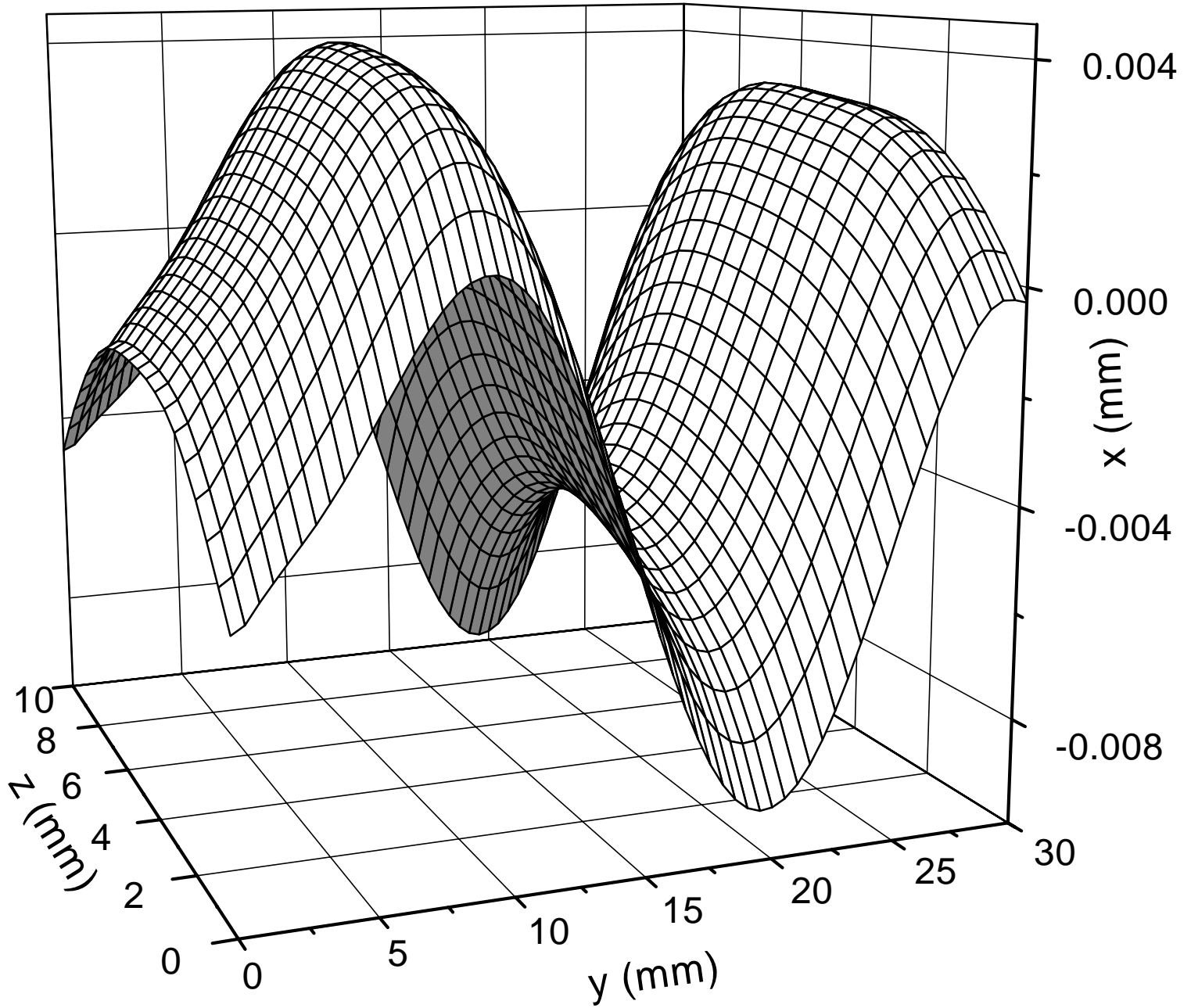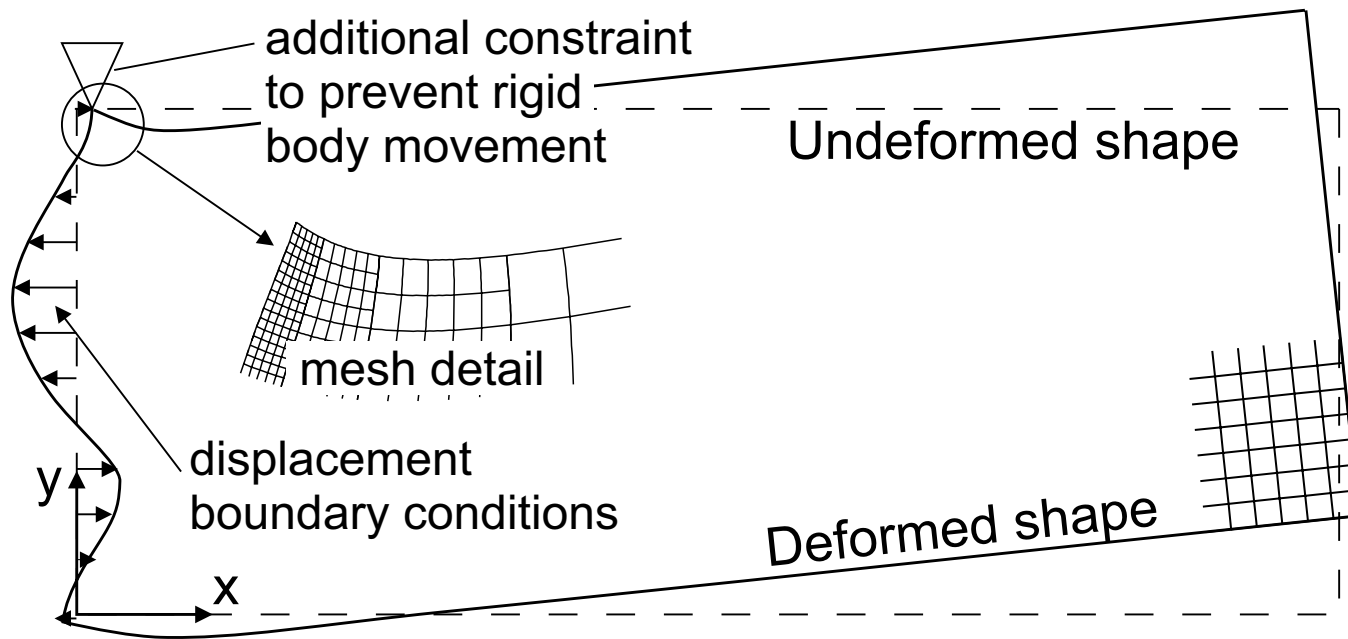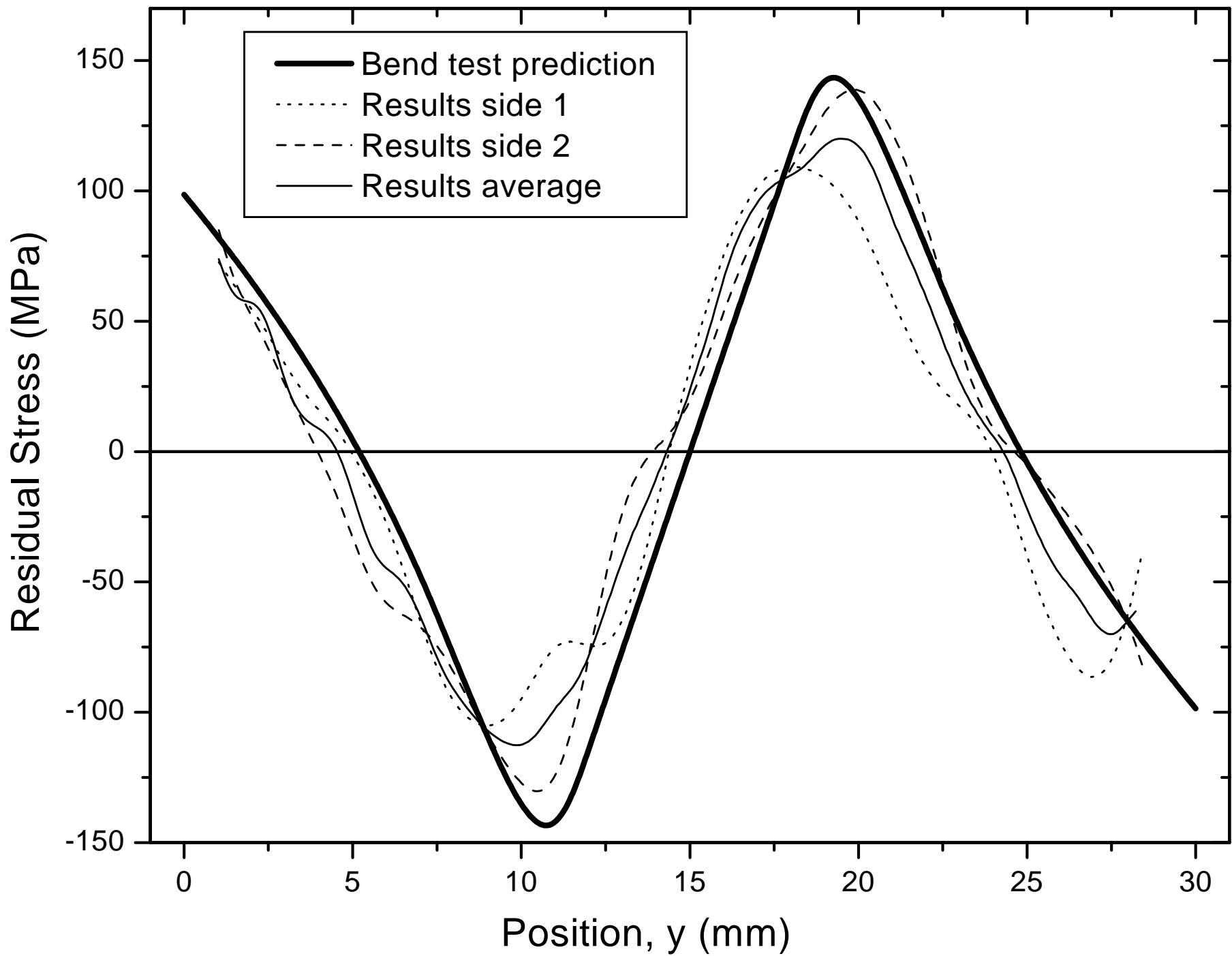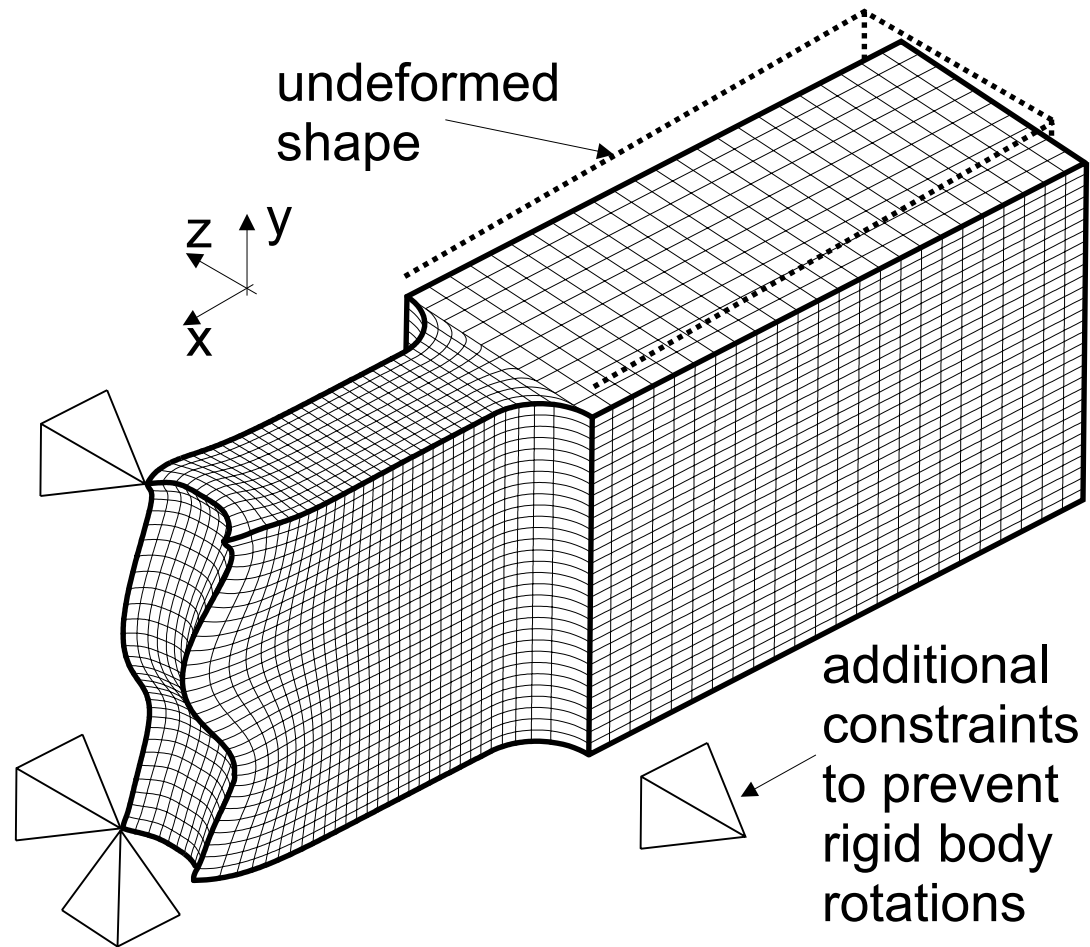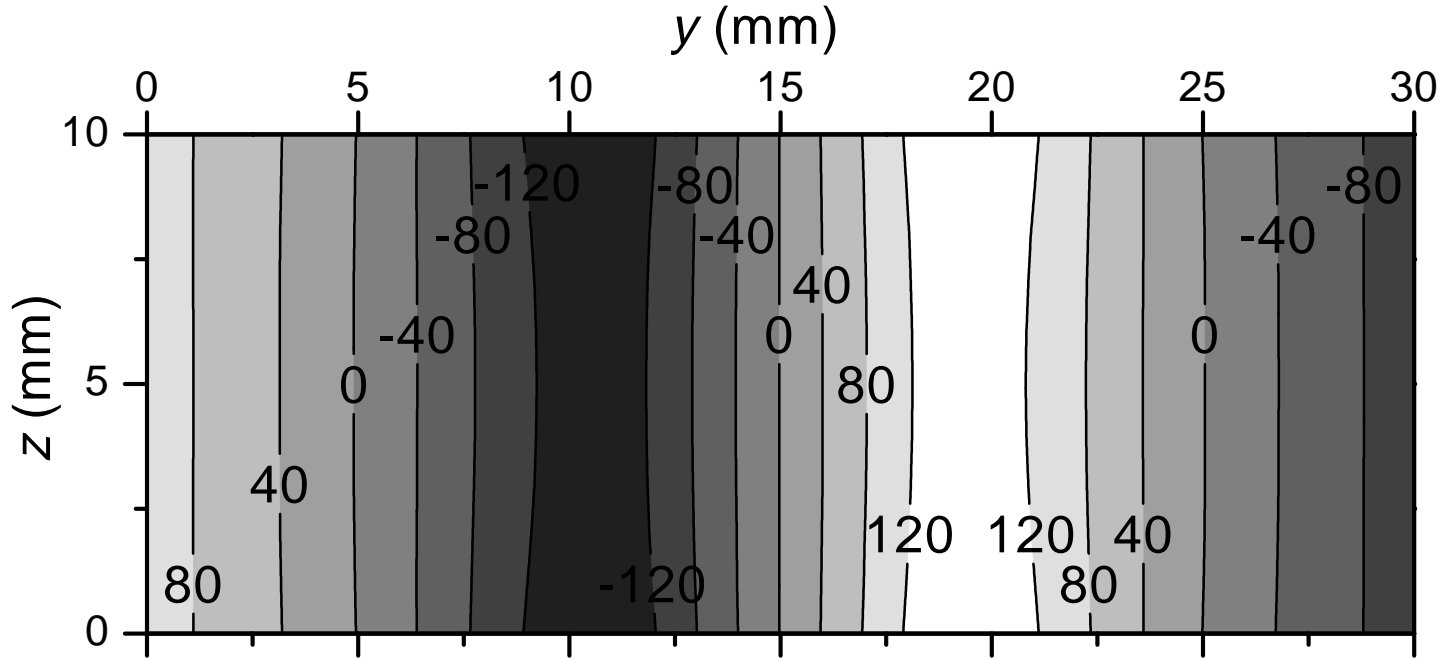
Prime Fig. 11

a. Bend test prediciton.
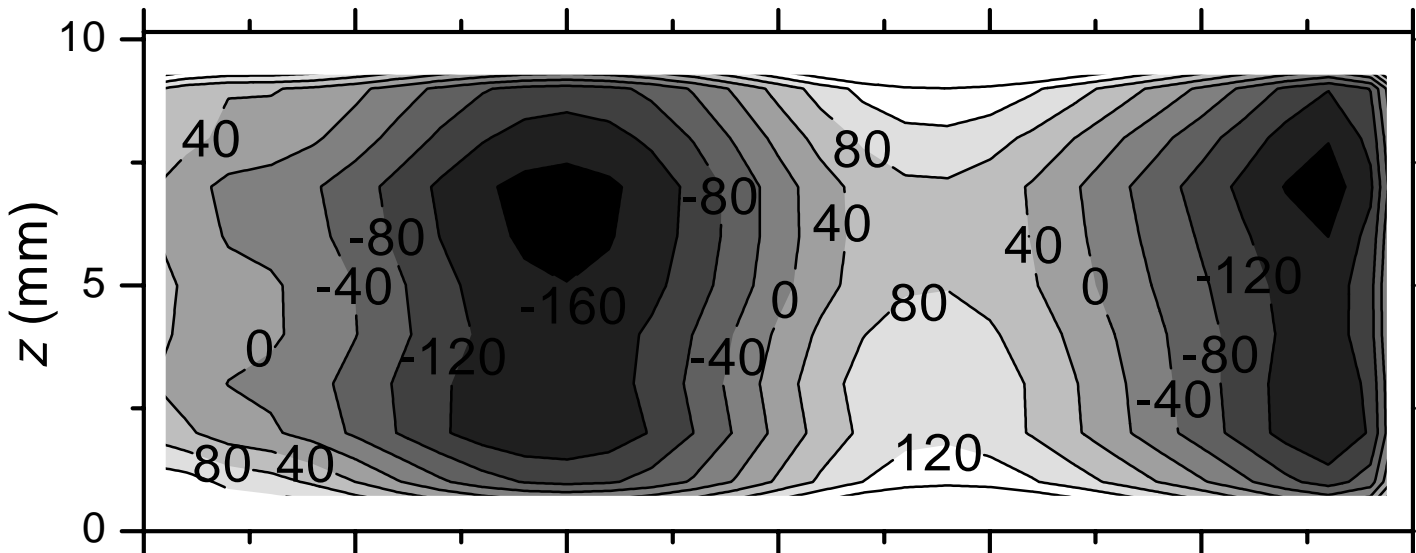
b. Uncorrected contour results.
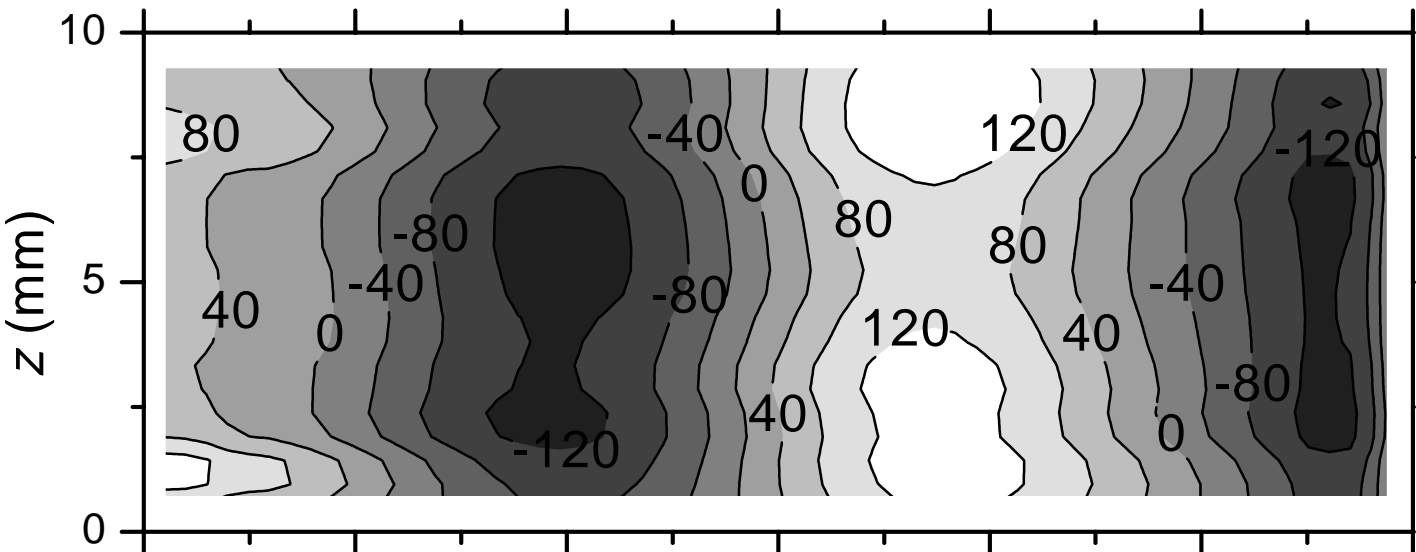
c. Corrected contour results.

Prime Figure 13